PHYSICAL REVIEW B VOLUME 27, NUMBER 7 1 APRIL 1983

Charged-particle wake in the random-phase approximation

A. Mazarro
Fisica del Estado Solido, Faculdad de Ciencias, University of Barcelona, Barcelona, Spain

P. M. Echenique and R. H. Ritchie*
Cavendish Laboratory, Madingley Road, Cambridge CB3 OHE, England
(Received 4 June 1982)

A study has been made of the wake of a swift charged particle in an electron gas using the full random-phase-approximation dielectric function of this medium. Our earliest work using the plasmon-pole approximation to the dielectric function gives a good account of most aspects of the wake when the velocity of the particle is greater than the Fermi velocity.

INTRODUCTION

Research in the last several years has been concerned with the distribution in space and time of perturbations of electron motion in solids caused by the passage of swift charged particles. Bohr[1] referred to the phenomenon of coherent electron displacements in atoms due to the passage of a charged particle as the "wake" behind the particle and marked its boundary, loosely, by a cone whose angle of opening was not defined. However, he gave no information about the distribution in space and time of the oscillatory perturbations in electron motion forming the wake. Later Neufeld and Ritchie[2] gave an explicit expression for the wake potential.

One had to wait until the early 1970's to see a renewal of the interest on the wake of charged particles in condensed matter. Neelavathi, Ritchie, and Brandt[3] (NRB) pointed out that the oscillatory wake of electron density fluctuations trailing a fast ion may (a) influence the motion of nearby ions traveling with nearly the same velocity and (b) give rise to wake-bound states. Subsequently Brandt, Ratkowski, and Ritchie[4] showed experimentally and theoretically that the energy loss of proton clusters in solids is influenced by the presence of such wakes. Following this, Gemmell *et al.*[5] found that it was necessary to include in their calculations the wake potential generated by the leading ion in order to explain the experimental distributions in energy and angle of protons emerging from crystals bombarded with $(HeH)^+$ beams under planar channeling conditions.

Recent experiments[6] on coherent resonant excitation of electrons in tightly bound K orbitals centered on nearly stripped, highly charged channeled ions are also sensitive to the presence of wake patterns of density fluctuations in the valence-electron sea of the crystal in which channeling occurs. Hybridization of excited hydrogenic levels on the ion (wake energy splitting) is a measure of the mean retarding force on the ion and has its origin in the wake.[7,8] Bell and co-workers[9] have measured the shift in the x-ray energy corresponding to the transition between the $^1P_1$ and $^1S_0$ multiplets in heliumlike sulfur projectiles. This shift can be explained as due to the decrease, caused by the wake, in binding energy of bound electronic states on the moving ion.[8]

The first calculation of the wake was made by Neufeld and Ritchie[2] using, for emphasis and simplicity, a local dielectric function to represent the response of the medium. They also studied the shock-wave aspects of the wake by employing a spatially dispersive dielectric function. The local form was also used in the first papers by NRB and Gemmell *et al.*[5] Day[10] suggested that inclusion of plasmon dispersion could vitiate some of NRB's conclusions about wake-riding states. More detailed calculations[11–13] did not bear out this suggestion, however. Ritchie *et al.*[11] used the plasmon-pole approximation to estimate the binding energy of wake-riding states. A detailed study of the wake potential and of the density fluctuations within the plasmon-pole approximation has been made recently by Echenique, Ritchie, and Brandt[12] and by Echenique and Ritchie.[13] Gemmell and co-workers have initiated an extensive program of research in the physics of molecular ions,[14] the theoretical interpretation of which involves the wake as a central concept.

In view of the importance and relevance of the wake concept in current experimental physics, it would be useful to have a detailed calculation of the wake potential and density fluctuations using the full random-phase-approximation (RPA) dielectric function to represent the response of the medium.

The results of such a calculation are presented in this paper. Besides their intrinsic interest, they provide a check of the validity of the plasmon-pole approximation for these problems. We also display, for the first time, the evolution of the wake potential as the velocity of the charged particle increases from values such that plasmon creation is impossible to higher velocities. The use of complete RPA quantum dielectric function allows us to present results for velocities smaller than the Fermi velocity of the electron gas. Although the use of linear theory for the medium's response may lead to some error, nonlinear treatments encounter difficulties such that only the static case has been treated.[15] Calculations of wake states binding energies are also presented.

THE WAKE IN RPA

The wake potential (i.e., the scalar electric potential) $\Phi_w(\vec{r},t)$ in an homogeneous isotropic medium due to a swift point charge Ze having constant velocity $\vec{v}$ is given by

$$\Phi_w(\vec{r},t)=\frac{2Ze}{\pi v}\int_0^\infty \kappa J_0(\kappa b)d\kappa\int_0^\infty \frac{d\omega}{\kappa^2+\omega^2/v^2}\mathrm{Re}\left[e^{i\omega\tilde{z}/v}\left[\frac{1}{\epsilon(k,\omega)}-1\right]\right]. \tag{1}$$

The cylindrical coordinates b and $\tilde{z}$ refer to the direction of motion and are defined as $b=(x^2+y^2)^{1/2}$ and $\tilde{z}=z-vt$ relative to the position $(x,y,z)=(0,0,vt)$ of the moving charge. The wave number

$$k=\left[\kappa^2+\frac{\omega^2}{v^2}\right]^{1/2}$$

has component κ in the b direction. The bare potential of the ion *in vacuo* has been subtracted from the total scalar potential in Eq. (1). The induced electron density fluctuation $\delta n(\vec{r},t)=\rho_{\mathrm{ind}}(\vec{r},t)/(-e)$ in the medium is related to Φ_w by Poisson's equation and is given by

$$\delta n(\vec{r},t)=-\frac{Z}{2\pi^2 v}\int_0^\infty \kappa J_0(\kappa b)d\kappa\int_0^\infty d\omega\,\mathrm{Re}\left[e^{i\omega\tilde{z}/v}\left[\frac{1}{\epsilon(k,\omega)}-1\right]\right]. \tag{2}$$

Lindhard[16] has derived the dielectric response function $\epsilon(k,\omega)$ in the RPA.[17] In terms of the dimensionless energy transfer $x=\omega/E_F$ and momentum transfer $y=k/2k_F$, where E_F and k_F are the Fermi energy and the Fermi momentum, the complex dielectric response function can be written as

$$\epsilon(k,\omega)=1+\frac{\chi^2}{y^2}[f_1(y,x)+if_2(y,x)]=\tilde{\epsilon}(y,x), \tag{3}$$

where $\chi^2=(\pi v_F)^{-1}$ and v_F is the Fermi velocity. We use atomic units in the rest of this paper. The real part $f_1(y,x)$ is given by

$$f_1(y,x)=\frac{1}{2}+\frac{1}{8y}\left[1-\left[y-\frac{x}{4y}\right]^2\right]\ln\left|\frac{y-\frac{x}{4y}+1}{y-\frac{x}{4y}-1}\right|+\frac{1}{8y}\left[1-\left[y+\frac{x}{4y}\right]^2\right]\ln\left|\frac{y+\frac{x}{4y}+1}{y+\frac{x}{4y}-1}\right|, \tag{4}$$

while the different representations of $f_2(y,x)$ which are to be employed in the regions of the (y,x) plane are

$$f_2(y,x)=\begin{cases}\pi x/8y & \text{in I } [0<x<4y(1-y)]\\ \dfrac{\pi}{8y}\left[1-\left[y-\dfrac{x}{4y}\right]^2\right] & \text{in II } [4y(\,|1-y|\,)<x<4y(1+y)]\\ 0 & \text{in III } [0<x<4y(y-1)] \text{ and IV } [4y(1+y)<x]\,.\end{cases} \tag{5}$$

In region III it is understood that $y\geq 1$.

The plasmon line $x=x_0(y)$ is defined as the set of points belonging to the region in which $\hat{\epsilon}(y,x)$ vanishes and for which $x>4y(1+y)$. The straight line $x=4vy/v_F$, corresponding to momentum and energy conservation, defines a point on the plasmon line and on the $x=4y(1+y)$ line whose corresponding abscissas we call y_1 and y_2, respectively.

In order to obtain the wake potential and the induced density fluctuation in the RPA, Eq. (3) is to be substituted into Eqs. (1) and (2). Confining ourselves to the wake potential, for the moment, we obtain

$$\Phi_w(\vec{r},t)=\Phi_w^c(\vec{r},t)+\Phi_w^s(\vec{r},t)\ ,$$

$$\Phi_w^c(\vec{r},t)=-\frac{Zv_F^2}{\pi v}\int_0^\infty\frac{dy}{y}\int_0^{4v_y/v_F}dx\,J_0(\alpha,b)[\chi^2 f_1(y^2+\chi^2 f_1)+\chi^4 f_2^2]\frac{\cos\gamma\tilde{z}}{F(y,x)}\ , \tag{6}$$

$$\Phi_w^s(\vec{r},t)=\frac{Zv_F}{\pi^2 v}\int_0^\infty y\,dy\int_0^{4v_y/v_F}dx\,J_0(\alpha,b)f_2\frac{\sin\gamma\tilde{z}}{F(y,x)}\ ,$$

where

$$\alpha=\left[4v_F^2y^2-\frac{v_F^4x^2}{4v^2}\right]^{1/2}\ ,$$

$$\gamma=\frac{v_F^2x}{2v}\ ,$$

and

$$F(y,x)=[y^2+\chi^2 f_1(y,x)]^2+\chi^4 f_2^2(y,x)\ .$$

We note that at least part of regions I, II, and III always contribute to the integration domain while only if $v>v_F$ is there a contribution from region IV. Likewise, part of the plasmon line belongs to it if $v>v_F(1+y_2)$.

Since the function $F(y,x)$ appearing in both integrands vanishes on the plasmon line, contributions to Φ_w^c and Φ_w^s arising from regions I, II, and III require straightforward use of Eqs. (4) and (5). Region IV demands special consideration. We define Φ_w^{sIV} to be the contribution from region IV to Φ_w^s.

On the plasma resonance line $x=x_0(y)$ one may write, considering f_2 to be a positive infinitesimal,

$$f_2/F=\pi\delta(y^2+\chi^2 f_1)/\chi^2=\frac{\pi^2 v_F\delta(x-x_0(y))}{\left|\frac{\partial}{\partial x}(y^2+\chi^2 f_1)_{x=x_0(y)}\right|}\ . \tag{7}$$

Accordingly, the Φ_w^{sIV} y integrand is reduced to the interval $[y_1,y_2]$ and the x integration may be immediately performed upon use of Eq. (7).

The contribution to Φ_w^c from region IV is a bit more complicated. We note it presents no problems except close to the plasmon line since then

$$\frac{1}{F}[\chi^2 f_1(y^2+\chi^2 f_1)+\chi^4 f_2^2]\underset{f_2\to 0}{\to}\frac{\chi^2 f_1}{y^2+\chi^2 f_1}\to\frac{1}{0} \tag{8}$$

must be interpreted as a principal value integral. The integral is of the type

$$I=\int_c^d dy\int_a^b dx\frac{P(y,x)}{G(y,x)}\ , \tag{9}$$

where if $y_1\le y\le y_2$ then $G(y,x=x_0(y))=0$ while $P(y,x=x_0(y))=0$. We write

$$I=\left[\int_c^{y_1}dy+\int_{y_1}^{y_2}dy+\int_{y_2}^{d}dy\right]\int_a^b dx\frac{P}{G} \tag{10}$$

and confine our attention to the second term which we rewrite as

$$I_2=\int_{y_1}^{y_2}dy\left.\frac{P(y,x)}{\frac{\partial G}{\partial x}}\right|_{x=x_0(y)}\ln\left[\frac{b-x_0}{x_0-a}\right]+\int_a^b dx\left[\frac{P}{G}-\left.\frac{P}{\frac{\partial G}{\partial x}}\right|_{x=x_0(y)}\right]. \tag{11}$$

For points close enough to the plasmon line, $x\simeq x_0(y)$,

$$G(y,x)=[x-x_0(y)]\left.\frac{\partial G}{\partial x}\right|_{x=x_0} \tag{12}$$

and the x integration in (11) becomes for those points

$$\int_a^b dx\frac{P(y,x)-P(y,x=x_0(y))}{x-x_0(y)}\ . \tag{13}$$

A criterion is given so as to decide whether or not a (y,x) point is close enough to the plasmon line, and in that case, the substitution

$$x-x_0\to\frac{x-x_0}{|x-x_0|}\epsilon\ \text{ if } x\neq x_0\qquad\to\epsilon\ \text{ if } x=x_0 \tag{14}$$

is made, where ϵ is a small positive constant value.

We can summarize our treatment of integral (9) as follows:

$$I=\int_0^d dy\left[S_0C_0+\int_a^b dx\left[\frac{P(y,x)}{G(y,x)}-\frac{S_c}{x-x_0}\right]\right]\ , \tag{15}$$

where

$$S_0=\begin{cases}\left.\dfrac{P(y,x)}{\frac{\partial G}{\partial x}}\right|_{x=x_0(y)} & \text{if } y_1\le y\le y_2\\ 0 \text{ otherwise}\ ,\end{cases}$$

$$C_0=\begin{cases}\ln\left[\dfrac{b-x_0}{x_0-a}\right] & \text{if } y_1\le y\le y_2\\ 0 & \text{otherwise .}\end{cases}$$

Our procedure (15) must be completed by substitutions (12) and (14) for points close enough to the plasmon line.

Our final result for the different contributions arising from regions I, II, III, and IV to Φ_w^c and Φ_w^s is given by

$$\Phi_W^{cI}(b,\tilde{z})=\frac{-4Z\tilde{v}v_F}{\pi}\int_0^{\min(1,v/v_F)}dl\int_0^{1-l}dy\,J_0(\alpha b)\cos\gamma\tilde{z}F_1\ ,$$
$$\Phi_w^{sI}(b,\tilde{z})=\frac{4Z\tilde{v}v_F}{\pi}\int_0^{\min(1,v/v_F)}dl\int_0^{1-l}dy\,J_0(\alpha b)\sin\gamma\tilde{z}F_2\ , \tag{16a}$$

$$\begin{Bmatrix}\Phi_w^{cII}(b,\tilde{z})\\ \Phi_w^{sII}(b,\tilde{z})\end{Bmatrix}=\frac{2Z\tilde{v}v_F}{\pi}\int_0^{\min[1,(2v/v_F)-1]}dt\int_1^{2v/v_F-t}ds\,J_0(\alpha b)\begin{Bmatrix}-\cos\gamma\tilde{z}F_1\\ \sin\gamma\tilde{z}F_2\end{Bmatrix}, \tag{16b}$$

$$\Phi_w^{cIII}(b,\tilde{z})=\frac{-2Z\tilde{v}v_F}{\pi}\int_0^1 d\tau\int_{-t}^{2v_F/v-t}ds\,J_0(\alpha b)\cos\gamma\tilde{z}\frac{q_1t^2}{\pi v_F(s-t)^3+q_1}\ ,$$
$$\Phi_w^{sIV}(b,\tilde{z})=\frac{2Z\tilde{v}v_F}{\pi}\int_{y_1}^{y_2}dy\,J_0(\alpha b)\left|_{l=l_0}\sin\gamma\tilde{z}\frac{16y^2\pi^2v_F}{\dfrac{\partial q_1}{\partial l}}\right|_{l=l_0}\ , \tag{16c}$$

$$\Phi_w^{cIV}(b\tilde{z})=-\frac{2Z\tilde{v}v_F}{\pi}\int_0^{v/v_F-1}dy\left[S_0C_0+\int_{1+y}^{v/v_F}dl\left[\frac{2J_0(\alpha b)\cos\gamma\tilde{z}q_1}{\pi v_F(s-t)^3+q_1}-\frac{S_0}{l-l_0}\right]\right],$$

where

$$F_1=\frac{q_1[\pi v_F(s-t)^3+q_1]+q_{2I}^2}{[\pi v_F(s-t)^3+q_1]^2+q_{2I}^2}\ ,$$
$$F_2=\frac{\pi v_F(s-t)^3q_{2I}}{[\pi v_F(s-t)^3+q_1]^2+q_{2I}^2}\ , \tag{16d}$$
$$S_0=\begin{cases}\left.\dfrac{2J_0(\alpha b)\cos(\gamma\tilde{z})q_1}{\dfrac{\partial q_1}{\partial l}}\right|_{l=l_0} & \text{if } y_1\le y\le y_2\\ 0 & \text{otherwise}\end{cases}$$
$$C_0=\begin{cases}\ln\left[\dfrac{v/v_F-l_0}{l_0-1-y}\right] & \text{if } y_1\le y\le y_2\\ 0 & \text{otherwise .}\end{cases}$$

As apparent in (16), some variable changes have been made to facilitate the calculations. They are

$$l=x/2y,\quad s=y+x/4y\ ,$$
$$t=-y+x/4y,\quad \tau=-1/t\ . \tag{17}$$

Also, we have

$$q_1(s,t)=4(s-t)f_1(s,t)\ ,$$
$$q_2(s,t)=4(s-t)f_2(s,t)\ ,$$
$$\tilde{v}=v/v_F\ .$$

Our wake potential $\Phi_w(\vec{r},t)$ is finally obtained as the sum of all these contributions:

$$\Phi_w=\Phi_w^{cI}+\Phi_w^{sI}+\Phi_w^{cII}+\Phi_w^{sII}+\Phi_w^{cIII}+\Phi_w^{sIII}+\phi_w^{cIV}\ .$$

To compute the induced density fluctuation δn we can follow a similar procedure since

$$\delta n(k,\omega)=-\frac{k^2}{4\pi}\Phi_{\rm ind}(k,\omega) \tag{18}$$

with corresponding multiplicative factors under the integrals over x and y.

WAKE POTENTIAL AND DENSITY FLUCTUATIONS

The well-defined oscillatory behavior of the wake potential behind the ion constitutes its outstanding feature. The way it changes as the ion velocity increases is shown in Figs. 1 and 2. The potential remains nearly constant when $v\lesssim v_F$ ($v_F=0.96$ for $r_s=2$ in our example). Only a slightly growing

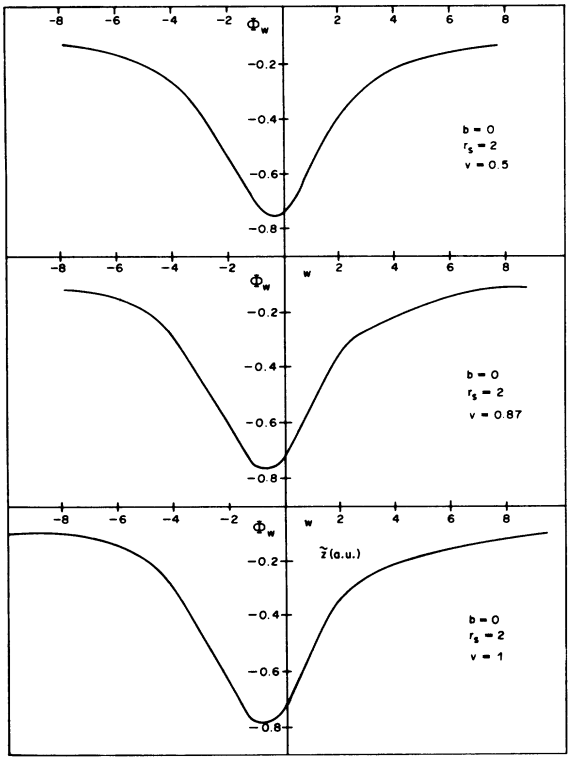

FIG. 1. Wake potential in the neighborhood of a proton moving in an electron gas at the aluminum density ($r_s=2$). The potential is plotted as a function of distance along the track for three different velocities less than the Fermi velocity in Al. All quantities are measured in atomic units.

asymmetry and a slighter well-depth growth is observed. However, once the Fermi velocity is exceeded, rapid changes take place as Fig. 2 illustrates. For $v > v_f(1+y_2)$ ($v > 1.32$ in our case), one can already see electron troughs in the wake potential. As expected from the NRB work, we find oscillatory behavior and plasmon creation closely related.

Figure 3 illustrates the variation of $-\Phi_w$ in the neighborhood of $\tilde{z}=\tilde{z}_0$, the position of the first trough for electron capture, for several different velocities. The curves labeled $\tilde{z}$ show $-\Phi_w(0,\tilde{z}-\tilde{z}_0)$ vs $\tilde{z}-\tilde{z}_0$, and the curves labeled b show $-\Phi_w(b,\tilde{z}_0)$ vs b. One sees that this trough evolves from a figure flattened in the direction of motion at the smaller values of v to a shape elongated in the direction of motion at larger v. This behavior is not described well in the NRB approximation since there the extensions of the first wake trough in the two directions both scale with v/ω_p. However, the plasmon-pole results of Echenique, Ritchie, and Brandt (ERB) are in general accord with this.

We have studied trends exhibited at still higher ion velocities and in different media. Figure 4 shows the variation of the wake potential behind the ion for several ion velocities. Distance $\tilde{z}$ along the particle track is scaled by the length v/ω_p so that the NRB wavelength is 2π. All curves take the value $\Phi_w=\pi\omega_p/2v$ just on the ion ($b=\tilde{z}=0$) as in the NRB (Ref. 3) and Ritchie, Brandt, and Echenique[11]- (RBE) ERB (Ref. 12) cases. In our work the wavelength is somewhat smaller than 2π decreasing with decreasing ion velocity.

Figure 5 shows the wake potential on axis as com-

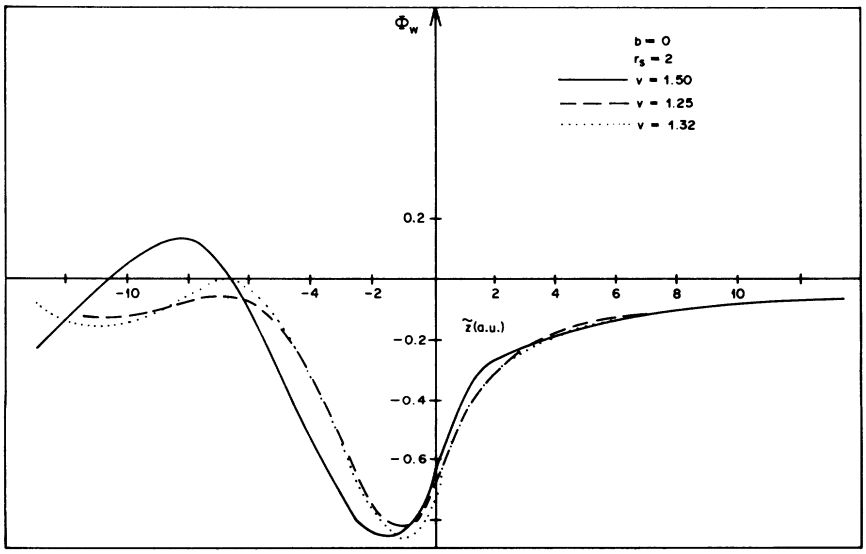

FIG. 2. Wake potential for the conditions of Fig. 1 and for three velocities larger than the Fermi velocity. The development of the oscillatory portion of the wake is clearly seen as the velocity increases.

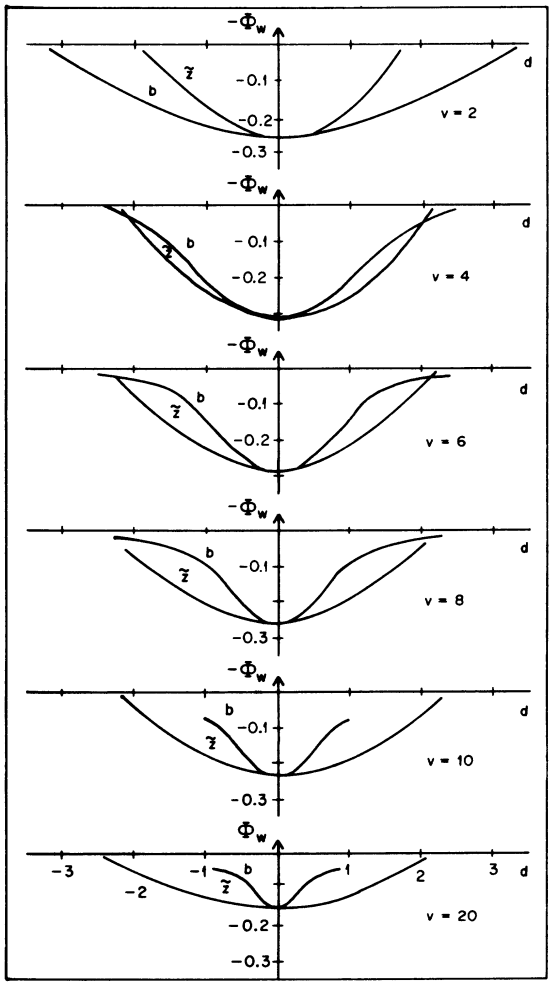

FIG. 3. Plots of the variation in the wake potential in the neighborhood of the first potential minimum for an electron. Data are presented for a proton moving with various velocities in an electron gas with $r_s=2$. The curves labeled b show the variation of $-\Phi_w$ with b, while those labeled $\tilde{z}$ show the variation with $\tilde{z}$. It seems that as v increases the profile of the trough changes from one that is flattened in the direction of motion to one that is elongated in the direction of motion.

puted from the local dielectric theory (with a cutoff) as in the work of NRB, from the plasmon-pole dielectric function by ERB, and from our RPA approach. This potential $\Phi_w(0,\tilde{z})$ vs $(\omega_p\tilde{z}/v)$ due to a proton with $v=4$ is multiplied by $(-v/\omega_p)$. The density of the electron gas was taken to be such that $r_s=4.0$. One sees that there is general agreement between the various results, with quite close matching of the wake potential in the RPA with that obtained from the plasmon-pole approximation.

Differences between our wake potential results and those of NRB, RBE, and ERB are presumably not important in most applications. We may add here our results do not appear to corroborate those of Stachowiak,[18] in that he obtains a screening until the ion velocity reaches approximately $0.8v_F$ with no screening at all for high ion velocities. This is in contradiction with our results pictured in Figs. 1 and 2.

We display the electron density fluctuation function $\delta n(0,\tilde{z})$ vs $\tilde{z}$ for different velocities of a proton in an electron gas for which $r_s=2.0$ in Figs. 6 and 7. No dramatic changes are involved for $v<v_f$. In particular, $v=0.01$ and $v=0.1$ curves are almost identical. It is interesting to compare δn with the static results of Langer and Vosko.[19] For $r_s=3$ value and at the ion position we find $\delta n/v_{F^3}\simeq 0.127$ for $v=0.01$ and $v=0.1$ compared with $\delta n/v_{F^3}\simeq 0.139$ from Langer and Vosko. Both of these results are much lower than the value obtained by Almbladh *et al.*[15] who include nonlinear terms in a calculation for the static case.

In Figs. 8 and 9 we show the fluctuation on the track of the charged particle when the wake is well established ($v=4$). Figure 8 shows the region behind the particle while Fig. 9 corresponds to the region ahead of the particle. In the latter the scale of $\tilde{z}$ is changed to enhance the small oscillatory contribution arising mainly from the single-particle response of the medium, as predicted by ERB. We note on the ion we get $\delta n=\omega_p^2/4v$ in agreement with the ERB treatment.

We illustrate in Fig. 10 the difference in the density fluctuation as computed in the plasmon-pole approximation and in our work. The inset shows in detail the region around the origin, while the larger set of axes shows a portion of the oscillatory region.

Figure 11 shows the density fluctuation in front of the ion for $v=4$ and two extreme values of electron density: $r_s=1.56$ and $r_s=6$. The wavelength of these fluctuations is medium independent and takes a value very close to $\pi/v\simeq 0.79$. Figure 12 shows the wake potential at the origin as a function of v compared with NRB and ERB's results.

WAKE BINDING ENERGIES

We have carried out a systematic numerical study of the wake potential near the minimum in the first potential trough for an electron behind the ion.[20] Numerical values of $\Phi_w(b,z)$ were fitted in the neighborhood of the minimum at $\tilde{z}=\tilde{z}_0$ by an expression of the form

$$-\Phi_w(b,\tilde{z})=-V_0+\alpha b^2+\beta(\tilde{z}-\tilde{z}_0)^2 . \qquad (19)$$

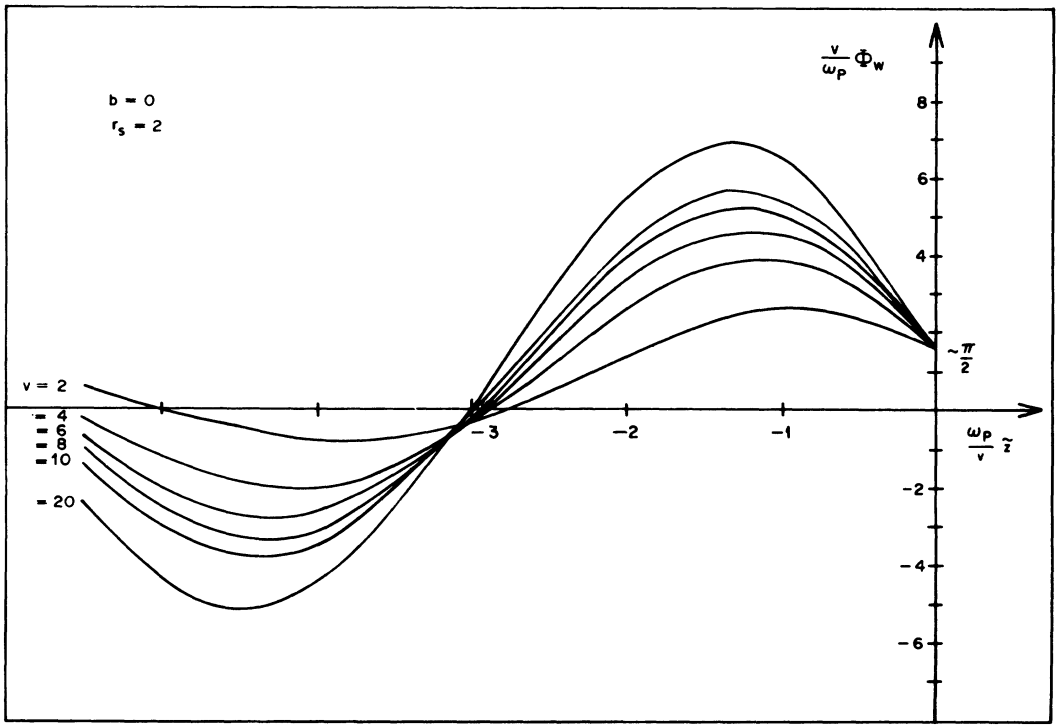

FIG. 4. Negative of wake potential plotted along the track for several different velocities. The distance behind the particle is scaled by the factor ω_p/v and the potential is scaled by the factor v/ω_p. In the simple NRB theory all these curves would be identical.

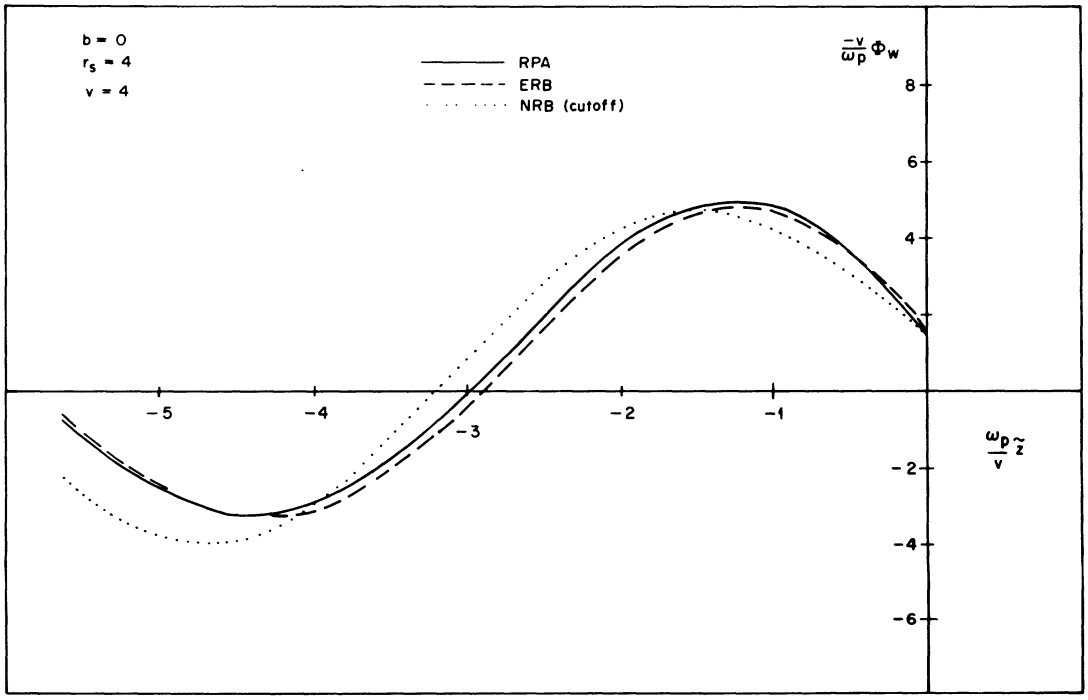

FIG. 5. Negative of the wake potential for $b=0$ plotted as a function of z behind a proton. Both Φ_w and $\tilde{z}$ are scaled as in Fig. 4. The three curves were obtained using various approximations to the dielectric function of the medium as explained in the text.

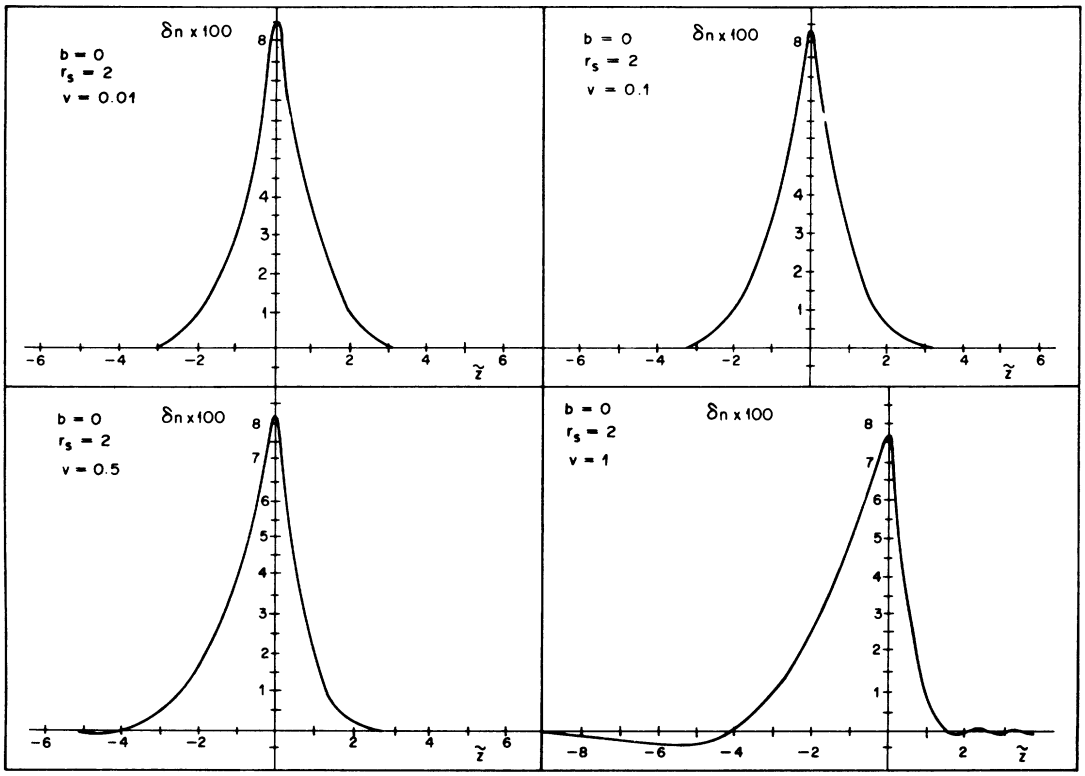

FIG. 6. Variation of the electron-density-fluctuation function with position along the track for several different proton velocities.

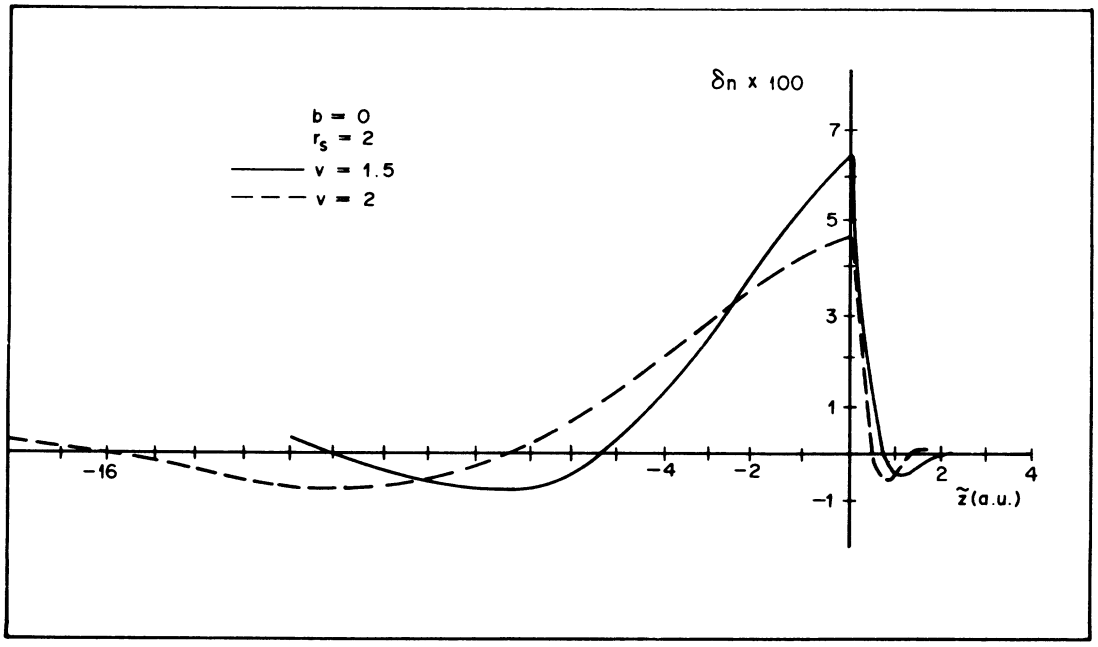

FIG. 7. Variation of the electron-density-fluctuation function with position along the track for two different velocities both larger than the Fermi velocity. The medium is an electron gas at a density corresponding to $r_s=2$.

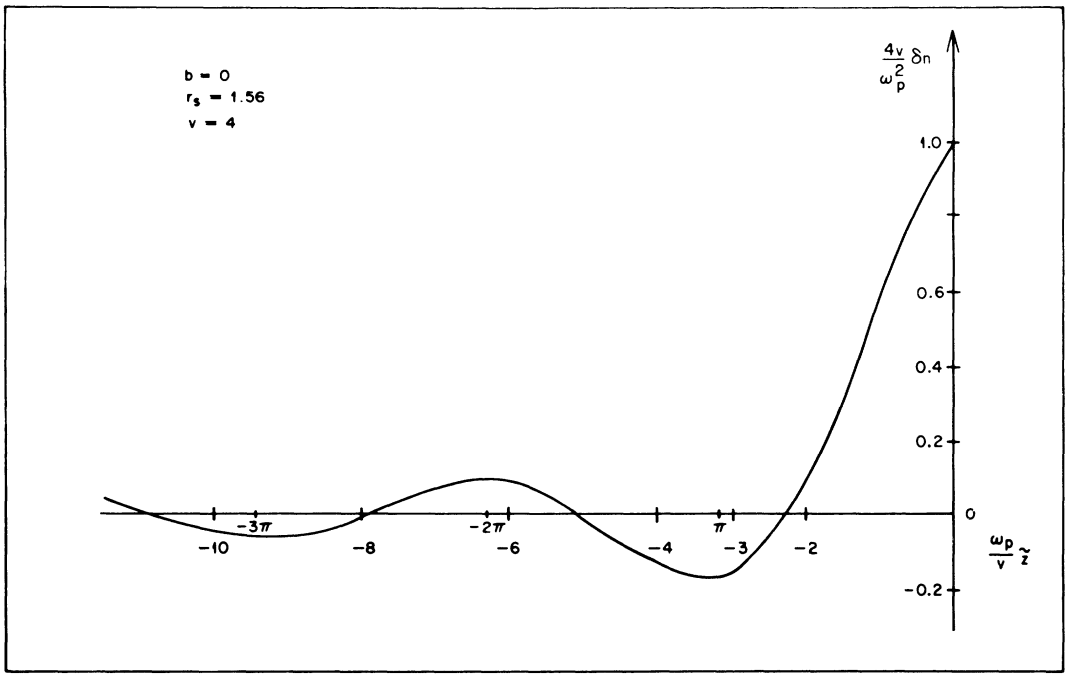

FIG. 8. Density-fluctuation function behind the proton for $r_s = 1.56$, $b = 0$, and at $v = 4$, where the wake is well established. Both δn and $\tilde{z}$ have been scaled in accordance with predictions of the plasmon-pole theory.

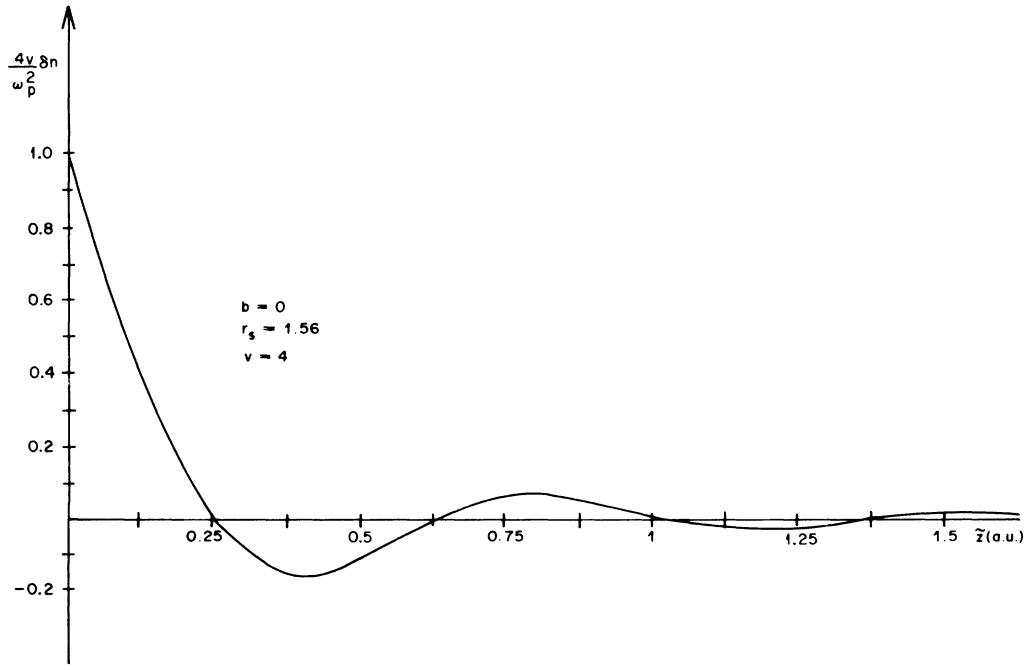

FIG. 9. Density-fluctuation function in front of the proton for the same conditions of Fig. 8, except that $\tilde{z}$ is given in atomic units to show the oscillations in δn clearly.

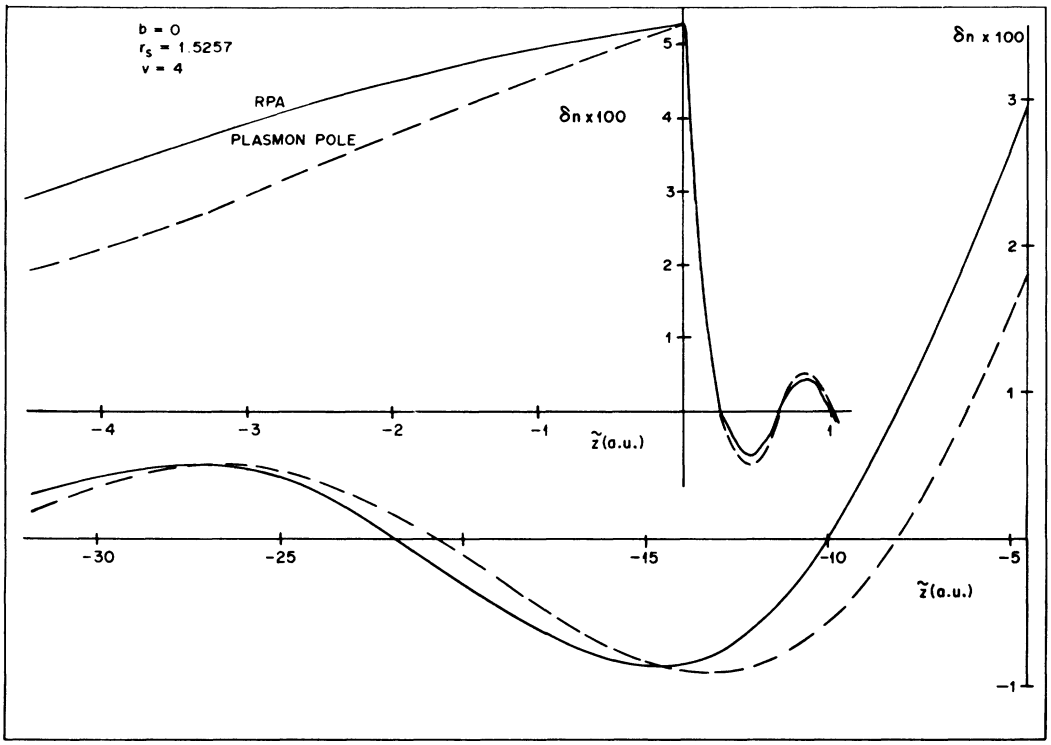

FIG. 10. Density-fluctuation function along the track of a particle for $r_s = 1.52$ and $v = 4$ computed in the RPA and in the plasmon-pole approximation. For clarity the curves have been presented on two separate contiguous sections of the z axis. It is seen that there are only minor differences in results obtained in the two approximations.

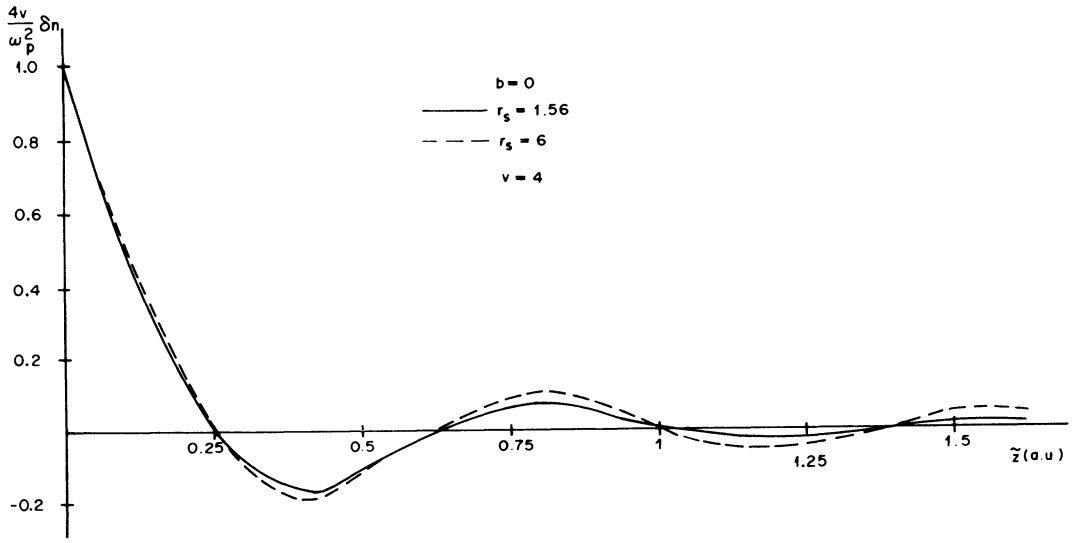

FIG. 11. Density fluctuation scaled by the factor $4v/\omega p^2$ plotted vs z for two quite different electron densities and for points ahead of the particle. Since δn in this region depends primarily on the single-particle response of the medium, the wavelengths and amplitudes are almost independent of the static electron density of the medium.

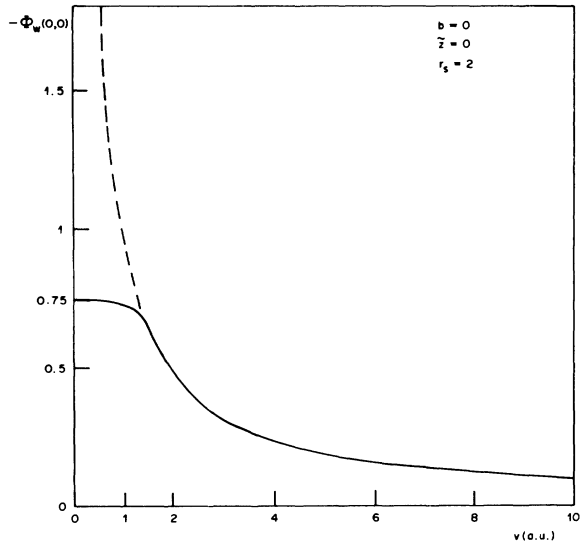

FIG. 12. Negative of the wake potential at $z=b=0$ as a function of the velocity of a proton in an electron gas at $r_s=2$. The solid curve shows the RPA results, while the dashed curve gives results obtained with the plasmon-pole approximation.

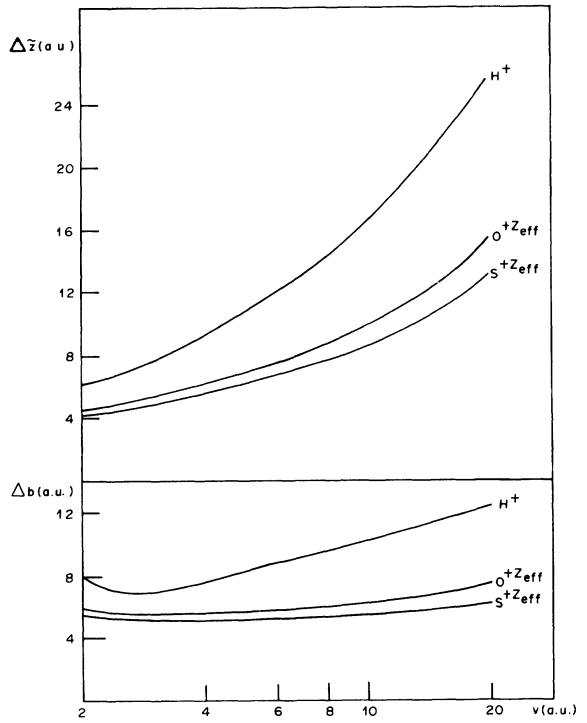

FIG. 13. Spatial extension of the ground-state wave function of an electron bound in the wake of various ions plotted as a function of ion velocity. The wave function is assumed to have the form $\psi\sim\exp[-(\tilde{z}-\tilde{z}_0)^2/(\Delta\tilde{z})^2-b^2/(\Delta b)^2]$, where $(0,\tilde{z}_0)$ is the position of the first minimum in the potential energy of an electron moving in the wake. The effective charge Z^{eff} of an ion with nuclear charge Z was computed from $Z^{\text{eff}}=Z_1(1-e^{-v/Z_1^{2/3}})$ when it has velocity v in atomic units. The electron-gas density corresponds to $r_s=2$.

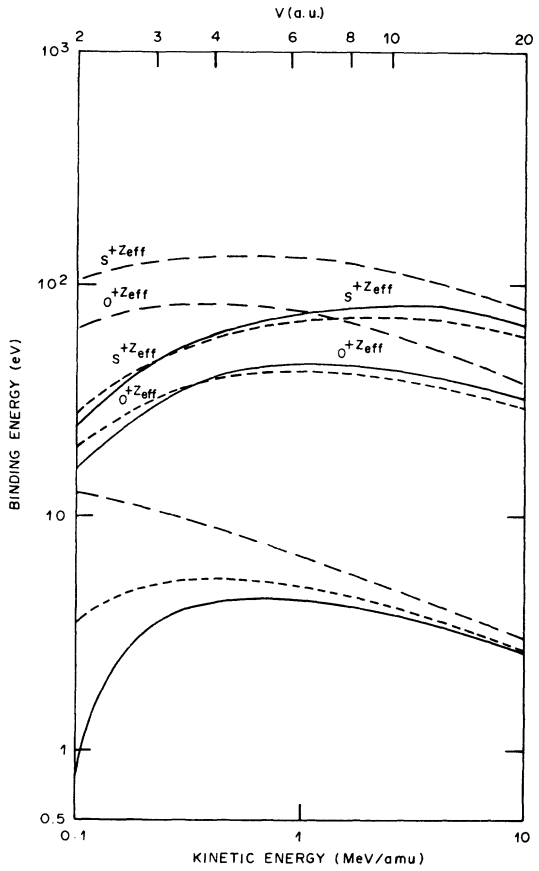

FIG. 14. Wave binding energies of electrons in their first potential trough plotted as a function of the energy of the leading ion. The three lower curves were computed assuming $Z_1=1$ while the ion is identified in the remaining curves. The solid curves were calculated in the RPA, the short-dashed curves were found using the plasmon-pole dielectric function, and the long-dashed curves were computed using the NRB method. The electron-gas density corresponds to $r_s=2$.

Electron binding energies in this harmonic-oscillator potential are found from standard quantum theory. Figure 13 shows the spatial extension of the wake-bound electron both in the longitudinal and transverse direction for three types of ions. Behind protons in the velocity range under discussion ($v=1-10$ a.u.) the wave function of the wake-bound electron extends over ($\sim 1-1.5$ a.u.). Figure 14 shows wake binding energies E_w in eV computed for protons oxygen and sulfur ions moving in an electron gas at a density corresponding to the conduction band in Al metal. The results are in general agreement with those found by Day and Ebel[21] who used a semiclas-

sical dielectric function to represent the response of the medium and a variational procedure in which an exponential trial function was employed. It might be noted that as more realistic dielectric functions are utilized, less wake binding of electrons is found at low speeds.

We have not included here the effect of the self-wake of the electron on its binding energy in the trough of a leading ion. This effect is estimated using a method described in RBE to result in an additional binding energy <1 eV for all cases studied here.

ACKNOWLEDGMENTS

Thanks are due to Professor Volker Heine and to Dr. A. Howie and Dr. John Inkson for their kind hospitality at the Cavendish Laboratory where part of this work was carried out. Very special thanks are due to C. M. M. Nex for his help and guidance with the numerical computations. One of us (R.H.R.) is grateful for a fellowship from the Royal Society. This work was sponsored in part by the Office of Health and Environmental Research, U.S. Department of Energy.

---

*Permanent address: Oak Ridge National Laboratory, Oak Ridge, Tenn. 37830 and Department of Physics, University of Tennessee, Knoxville, Tenn. 37916.

[1]N. Bohr, K. Dan. Vidensk. Selsk. Mat.-Fys. Medd. 18, No. 8 (1948).

[2]J. Neufeld and R. H. Ritchie, Phys. Rev. 98, 1632 (1955); 99, 1125 (1955).

[3]V. N. Neelavathi and R. H. Ritchie, *Atomic Collisions in Solids V* (Plenum, New York, 1975), p. 289; V. N. Neelavathi, R. H. Ritchie, and W. Brandt, Phys. Rev. Lett. 33, 302 (1974); 33, 670(E) (1974); 34, 560(E) (1975).

[4]W. Brandt, A. Ratkowski, and R. H. Ritchie, Phys. Rev. Lett. 33, 1325 (1974); 35, 130E (1975).

[5]D. S. Gemmell, J. Remillieux, M. J. Gaillard, R. E. Holland, and F. Vager, Phys. Rev. Lett. 34, 1420 (1975).

[6]S. Datz, C. D. Moak, O. H. Crawford, H. F. Krause, P. F. Dittner, J. Gomez del Campo, J. A. Biggerstaff, P. D. Miller, P. Hvelplund, and H. Knudsen, Phys. Rev. Lett. 40, 843 (1978).

[7]O. H. Crawford and R. H. Ritchie, Phys. Rev. A 20, 1848 (1979).

[8]J. Tejada, P. M. Echenique, O. H. Crawford, and R. H. Ritchie, Nucl. Instrum. Methods 170, 249 (1980).

[9]F. Bell, H. D. Betz, H. Panke, and W. Stehling, J. Phys. B 9, 3017 (1976); D. H. Jakubassa, J. Phys. C 10, 4491 (1977).

[10]M. H. Day, Phys. Rev. B 12, 514 (1975).

[11]R. H. Ritchie, W. Brandt, and P. M. Echenique, Phys. Rev. B 14, 4808 (1976); P. M. Echenique, Ph.D. thesis, University of Barcelona, 1977 (unpublished).

[12]P. M. Echenique, R. H. Ritchie, and W. Brandt, Phys. Rev. B 20, 2567 (1979).

[13]P. M. Echenique and R. H. Ritchie, Elhuyar 17, 1 (1979). This paper is written in Basque. Reprints may be obtained by writing to the journal editor of Elhuyar, Circulo San Ignacio, San Marcial 26 Bajo, S. Sebastian, Spain.

[14]See, e.g., *Proceedings of the Workshop on Physics with Fast Molecular-Ion Beams,* edited by D. S. Gemmell, Argonne National Laboratory Report No. ANL/PHY-79-3 (unpublished).

[15]C. O. Almbladh, U. von Barth, F. D. Popovic, and M. J. Scott, Phys. Rev. B 14, 2250 (1976).

[16]J. Lindhard, K. Dan. Vidensk. Selsk. Mat.-Fys. Medd. 28, No. 8 (1954).

[17]See, e.g., D. Pines and P. Noziéres, *Theory of Quantum Liquids* (Benjamin, New York, 1966).

[18]H. Stachowiak, Bull. Acad. Pol. Sci. 23, 1213 (1975).

[19]J. S. Langer and S. H. Vosko, J. Phys. Chem. Solids 12, 196 (1960).

[20]P. M. Echenique and R. H. Ritchie, Phys. Rev. B 21, 5854 (1980).

[21]M. H. Day and M. Ebel, Phys. Rev. B 19, 3434 (1979).